HHS Public Access

Author manuscript

ACS Appl Mater Interfaces. Author manuscript; available in PMC 2023 April 27.

Published in final edited form as:

ACS Appl Mater Interfaces. 2022 April 27; 14(16): 18935–18943. doi:10.1021/acsami.2c03110.

Stretchable Encapsulation Materials with High Dynamic Water Resistivity and Tissue-Matching Elasticity

Yan Shao,
Department of Materials Science and Engineering, University of Wisconsin-Madison, Madison, Wisconsin 53706, United States

College of Polymer Science and Engineering, Sichuan University, Chengdu 610065, P. R. China

Shan Yan,
Department of Materials Science and Engineering, University of Wisconsin-Madison, Madison, Wisconsin 53706, United States

Jun Li,
Department of Materials Science and Engineering, University of Wisconsin-Madison, Madison, Wisconsin 53706, United States

Zulmari Silva-Pedraza,
Department of Materials Science and Engineering, University of Wisconsin-Madison, Madison, Wisconsin 53706, United States

Department of Surgery, School of Medicine and Public Health, University of Wisconsin-Madison, Madison, Wisconsin 53706, United States

Ting Zhou,
Department of Surgery, School of Medicine and Public Health, University of Wisconsin-Madison, Madison, Wisconsin 53706, United States

Marvin Hsieh,
Department of Surgery, School of Medicine and Public Health, University of Wisconsin-Madison, Madison, Wisconsin 53706, United States

Bo Liu,
Department of Surgery, School of Medicine and Public Health, University of Wisconsin-Madison, Madison, Wisconsin 53706, United States

Tong Li,

Corresponding Author: Xudong Wang – xudong.wang@wisc.edu.

The authors declare no competing financial interest.

ASSOCIATED CONTENT

Supporting Information

The Supporting Information is available free of charge at https://pubs.acs.org/doi/10.1021/acsami.2c03110.

SEM images of PIB blend films, UV spectrum of PIB blend films, dynamic mechanical modulus of PIB blend films, temperature sweep of PIB blend films, setup for measuring the water transmission rate, combination of modulus and water permeability of PIB blend films, work mechanism of sliding-mode TENG, setup for measuring the voltage output, and setup for measuring the dynamic stability of packaged NGs (PDF)

Complete contact information is available at: https://pubs.acs.org/10.1021/acsami.2c03110

Department of Materials Science and Engineering, University of Wisconsin-Madison, Madison, Wisconsin 53706, United States

Long Gu,
Department of Materials Science and Engineering, University of Wisconsin-Madison, Madison, Wisconsin 53706, United States

Yunhe Zhao,
Department of Materials Science and Engineering, University of Wisconsin-Madison, Madison, Wisconsin 53706, United States

Yutao Dong,
Department of Materials Science and Engineering, University of Wisconsin-Madison, Madison, Wisconsin 53706, United States

Bo Yin,
College of Polymer Science and Engineering, Sichuan University, Chengdu 610065, P. R. China

Xudong Wang
Department of Materials Science and Engineering, University of Wisconsin-Madison, Madison, Wisconsin 53706, United States

College of Polymer Science and Engineering, Sichuan University, Chengdu 610065, P. R. China

Department of Surgery, School of Medicine and Public Health, University of Wisconsin-Madison, Madison, Wisconsin 53706, United States

Abstract

Flexible implantable medical devices (IMDs) are an emerging technology that may substantially improve the disease treatment efficacy and quality of life of patients. While many advancements have been achieved in IMDs, the constantly straining application conditions impose extra requirements for the packaging material, which needs to retain both high stretchability and high water resistivity under dynamic strains in a physiological environment. This work reports a polyisobutylene (PIB) blend-based elastomer that simultaneously offers a tissue-like elastic modulus and excellent water resistivity under dynamic strains. The PIB blend is a homogeneous mixture of two types of PIB molecules with distinct molecular weights. The blend achieved an optimal Young's modulus of 62 kPa, matching those of soft biological tissues. The PIB blend film also exhibited an extremely low water permittivity of 1.6–2.9 g m^{-2} day^{-1}, from unstrained to 50% strain states. The combination of high flexibility and dynamic water resistivity was tested using triboelectric nanogenerators (TENGs). The PIB blend-packaged TENG was able to stably operate in water for 2 weeks, substantially surpassing the protection offered by Ecoflex. This work offered a promising material solution for packaging flexible IMDs to achieve stable performance in a strained physiological environment.

Graphical Abstract:

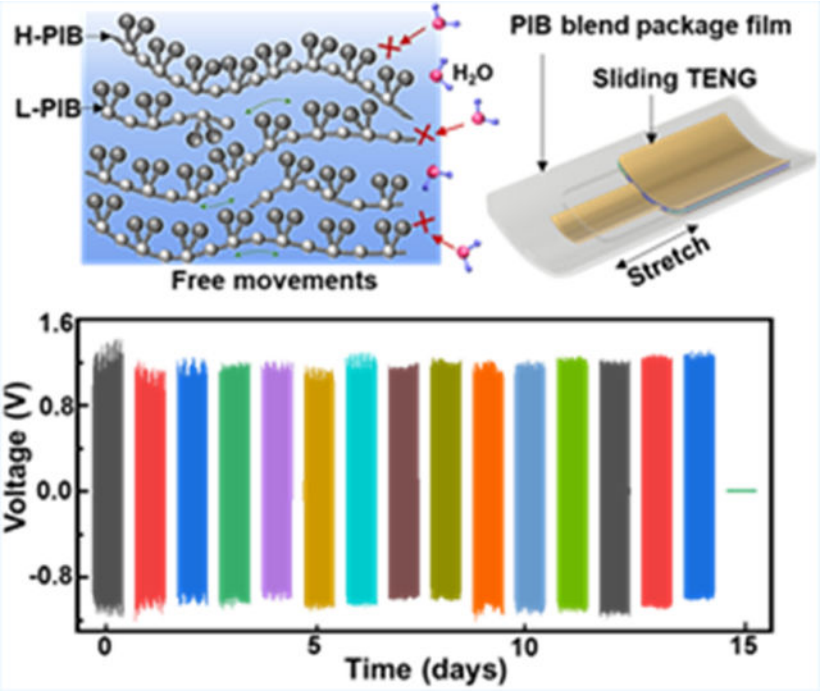

Keywords

polyisobutylene; flexible packaging; dynamic water resistivity; implantable medical devices; nanogenerators

INTRODUCTION

Implantable medical devices (IMDs) are rapidly evolving as a powerful component in modern biomedical systems. They are typically affixed on tissue or organ surfaces and provide continuous and in vivo monitoring, diagnosis, drug delivery, or therapeutic functions. Popular clinically available IMDs include pacemakers, cardiac defibrillators, cochlear implants, and implantable infusion pumps.[1–8] While most current IMDs are still rigid and metal-shelled bulk devices, the trend of IMDs is moving toward conformal, soft, stretchable, and even degradable systems.[9,10] New evolution of IMDs imposes new requirements for their properties. Due to their unique operation environment, the devices need to ideally process tissue-matching mechanical properties to reduce the risk of tissue injury and decrease burdens on organ functions.[11,12] Meanwhile the devices need to sustain their proper function when the physiological surrounding is dynamically curved, strained, or twisted. In addition, the physiological environment is typically full of liquid. It is critical to protect IMDs from exposure to the body liquid to achieve a stable operation as well as life-long safety in the body.

Encapsulation is an indispensable and effective way to protect IMDs from the physiological environment and thus sustain the desired life span in vivo. A complete encapsulation process can protect the IMD electronics from interacting with biofluids, prevent the device from corrosion, and minimize electricity leakage from the IMDs to biological

tissues. Nevertheless, most current encapsulation methods only consider static protection, i.e., the devices are not subjected to any physical movements. While encapsulation works for rigid IMDs, dynamic strains are often associated with flexible IMDs. Using implantable nanogenerators (NGs) as an example, it is a promising powering device that converts biomechanical motions into electrical energy in vivo. The operation of NGs requires constant straining actions to generate electricity. How to ensure good insulation of implantable NGs stands as a critical challenge for their practical applications. So far, poly(dimethylsiloxane) (PDMS) and Ecoflex are commonly used as the packaging material for NGs due to their good flexibility and biocompatibility.[13–15] However, due to the high permeability of water molecules, they are incapable of supporting the long-term in vivo operation of implantable NGs. To address this challenge, researchers have tried to deposit water-impermeable thin coatings such as metal oxides, Parylene, or hybrid multilayers onto the elastomer surfaces to provide an extra barrier against water infiltration.[16–19] Although these coating could improve water resistance of the flexible encapsulation, they inevitably increase the mechanical modulus of materials and induce much higher device stiffness compared to the hosting tissue. Furthermore, these additional layers often have much lower stretchability compared to the elastomer encapsulations. Continuous straining actions would easily create defects to these thin coatings and diminish their water resistivity. As a result, the actual improvement to the long-term stability of implantable NGs introduced by this approach is rather limited.

Therefore, it is essential and urgent to develop a new flexible packaging material or strategy that can satisfy all of the requirements simultaneously for in vivo dynamic operation of NGs or most flexible IMDs, particularly being able to retain a constantly high water resistivity under dynamic strains. Polyisobutylene (PIB), a Food and Drug Administration (FDA)-approved and commonly used food ingredient such as gum,[20] is known for its intrinsically low water permeability. The fully saturated nonpolar C–C backbone together with the alternative small methyl groups offers a unique possibility to achieve both low water permittivity and relatively high chain mobility simultaneously.[21,22] PIB can be formed in different molecular weights that span from liquid to solid with a wide range of mechanical modulus. In this work, a binary PIB blend-based packaging material was developed, where a high-molecular-weight PIB (H-PIB) was chosen as the matrix to form an entangled network to endow desired stretchable and elastic properties and the low-molecular-weight PIB (L-PIB) acted as a plasticizer to enhance the movement of molecule chains to decrease the elastic modulus. The modulus of the PIB blend film at the L- to H-PIB weight ratio of 6:4 demonstrated an elastic modulus of 62 kPa, matching those of most body tissues. This PIB blend film demonstrated excellent encapsulation performance in an aqueous environment under dynamic mechanical strains, allowing a packaged triboelectric NG (TENG) to operate continuously for 2 weeks in the water environment, substantially surpassing the protection offered by Ecoflex. This work offers an effective solution for packaging flexible IMDs to achieve long-term in vivo operations in the physiological environment.

RESULTS AND DISCUSSION

L-PIB (M_n:920) was blended with H-PIB (M_n:600 000) with a hypothesis that the PIB oligomers can facilitate the molecular chain mobility while still sustaining a close contact

of all molecules to keep PIB's good water barrier property (Figure 1a). The PIB blend films were prepared by casting a well-mixed PIB–hexane solution on a flat surface. The solid film was obtained after the solvent was completed evaporated (see Experimental Section for details). The film thickness could be controlled by applying more solution in the container, while there was no limitation on the size of the film, demonstrating excellent scalability of this preparation technique. No phase separation features can be seen from the film surfaces and cross sections, as revealed by the uniform contrast under scanning electron microscopy (SEM) (Figure S1), suggesting that L-PIB molecules could well distribute within the network of entangled long H-PIB molecular chains. As a result, the as-received PIB blend films exhibited uniformly high transparency (Figures 1b and S2). Fourier transform infrared (FTIR) spectroscopy was performed to analyze possible chemical structure alteration after blending. As shown in Figure 1c, both pristine H-PIB and PIB blend films showed the same characteristic absorption peaks of the PIB chains. No new peaks were observed from the PIB blend film, indicating that there were no new chemical interactions between the molecular chains of H-PIB and L-PIB. To confirm that the desired hydrophobicity of PIB was not changed after blending, water contact angles were measured and compared with those of the pristine H-PIB and PIB blend films. As shown in Figure 1d, both films exhibited a very close water contact angle at ~113°, confirming that short-chain L-PIB had negligible influences on the hydrophobic property, which is preferred for achieving good protection in the physiological environment.[23]

To gain insights into the blending ratio, PIB blend films were fabricated with different L-PIB to H-PIB weight ratios, ranging from 2:8 to 7:3. All of the films were made with the same thickness, and all exhibited similarly smooth and homogeneous surfaces with high transparency. As an essential property for flexible NGs, the film's mechanical properties were studied in correlation to the weight ratio. Figure 2a presents the stress–strain curves measured from all PIB blend films with an identical rectangular shape ($30 \times 7 \times 0.3$ mm^3) at a strain rate of 50 mm min^{-1}. For comparison, the same measurement was also conducted on the same-sized films of PDMS, Ecoflex, and medium molecular weight PIB (M-PIB, molecular weight ~200 000, which was close to the median of L-PIB and H-PIB). All of the PIB blends exhibited excellent stretchability and survived under large stains of at least 75%, suggesting that the integration of L-PIB did not jeopardize the integrity of long-chain PIB networks. All of the PIB blends showed a typical elastomer behavior. In general, the strength decreased as the content of L-PIB increased in the blends. The stress–strain relationships of all samples were mostly linear within the strain range of 0–30% and then slightly tapered off as strain further increased. The elastic modulus values of all of the samples were thus determined from the slope within the linear range (three samples for each blend ratio). As shown in Figure 2b, the elastic modulus of pristine H-PIB was ~400 kPa. As L-PIB was added, the moduli of PIB blend films decreased monotonically. When the weight ratio was 6:4, the modulus reached as low as 62 kPa. A further increase in the L-PIB content to 7:3 in the blend exhibited minimal impacts on the modulus. The introduction of short-chain L-PIB could reduce chain entanglement of H-PIB and enhance the chain mobility, thereby reducing the material modulus. The 6:4 ratio appeared to be the maximum point where the freedom of long-chain PIB could reach by L-PIB facilitation. Therefore, it is essential to blend two types of PIB with distinguishing molecular weights to achieve desired modulus

modification. For just one single type of PIB with a medium molecular weight that was similar to the average of the L-PIB and H-PIB at the weight ratio of 6:4, the interaction among molecules was still strong and the modulus (350 kPa) was only slightly smaller than that of H-PIB. Ecoflex and PDMS, as two benchmark packaging elastomers, had a modulus of 70 KPa and 1 MPa, respectively, within the measurement range, which could be reached and surpassed by the blends with a 6:4 weight ratio and above. Therefore, PIB blends with a 6:4 weight ratio were chosen in our further studies.

Because the operation of implantable NGs requires continuous straining actions, the dynamic mechanic properties need to be evaluated. The dynamic modulus of the blend film was tested under varying strains ranging from 1 to 7% at 1 Hz from two samples (both showed nearly identical results, Figure S3). As shown in Figure 2c, the storage modulus (~75 kPa) and loss modulus (~15 kPa) remained stable across the entire testing strain range, indicating that the PIB blend film was able to function normally under a consecutive straining condition. The substantially larger storage modulus compared to the loss modulus demonstrated that the film had a characteristic elastic property.[24] The repeating cycling test also presented a good reproducibility of the stress–strain curves of the PIB blend film (6:4), evidencing the film's stable mechanical property during multiple loading–unloading cycles (Figure 2d). To further evaluate the mechanical stability of the PIB blend film in an aqueous environment, the film was stretched repeatedly in water to a strain of 30% for 18 000 cycles at a frequency of 1 Hz. The stress–strain curves were measured before and after the endurance test. As shown in Figure 2e, identical mechanical behavior was obtained, confirming that the PIB blend film could retain high mechanical stability after a long-term stretching operation in water.

Temperature sweeps of the dynamic mechanical properties were then conducted to determine the glass transition temperature (T_g) within the temperature range from −90 to 0 °C at 1 Hz (Figure 2f). A sharp peak of tan δ was observed at −38 and −45 °C for pristine H-PIB and PIB blend (6:4), respectively, which corresponds to their T_g. The shift of T_g to lower temperatures indicates that blending L-PIB into H-PIB could improve segmental mobility. This could also be supported by the reduced storage modulus (E′) and loss modulus (E″) of the PIB blend compared to those of pristine H-PIB (Figure S4). In addition, only one T_g peak was identified from the PIB blend film, which also indicated the good homogeneity of PIB blend films. In addition, there was a shoulder peak located at −58 °C in the tan δ spectrum of pristine PIB, but not shown in that of the PIB blend (6:4). This shoulder peak can be attributed to the sub-Rouse modes.[25,26] Introducing L-PIB disrupted the chain packing of PIB, endowing larger motion units (the Rouse mode) with higher mobility. Thus, the Rouse mode had a tendency to shift toward the local segmental motion. As a result, the shoulder tan δ peak disappeared. This also evidenced that the introduction of L-PIB can improve the segmental mobility.

The essential function of the packaging material for implantable NGs is to prevent body fluid infiltration. The water permeability of all PIB blend films and a few commercial packaging elastomers was measured by the gravimetric method using glass vials filled with desiccant over a 3-weeks period (Figure S5). All of the film samples had the same thickness of 300 μm. Each sample was measured three times to obtain the mean values and standard

deviations. As shown in Figure 3a, the values of water permeability for Ecoflex and PDMS were found to be 260 and 230 g m^{-2} day^{-1}, respectively, whereas all of the PIB blend films exhibited water permeability at the level of ~1 g m^{-2} day^{-1}. The more than two orders of magnitude lower water permeability of the PIB blend can be attributed to the combined effect of the nonpolar C–C chain and dense small pendant methyl groups.[27] Compared to the silicon-based elastomers, the repeating C–CH_3 units offer weaker intermolecular interaction with water molecules and reduce their adsorption. In addition, the small and dense pendant methyl groups on the main C–C chain minimized the internal free volumes, further restricting the diffusion of water molecules.[21,28] The water permeability values for all PIB blend films increased and are shown in the inset of Figure 3a. The water permeability increased monotonically following the L-PIB ratio. The pristine H-PIB showed the lowest water permeability of 0.75 ± 0.14 g m^{-2} day^{-1}, which increased to 1.6 ± 0.18 g m^{-2} day^{-1} for the PIB blend film at 6:4. This result is intuitive because the short-chain L-PIB could facilitate the overall polymer chain motions and thus provide more accessible internal free volumes, allowing water molecules to diffuse through. Despite this small increment, the PIB blend film still substantially enhanced the water resistivity behavior compared to Ecoflex and PDMS. Considering both modulus and water permeability, the PIB blend film (6:4) demonstrated the first combination of both properties (Figure S6) and was selected for further study and packaging applications. Considering the devices need to work under dynamic straining conditions, the water permeability of the PIB blend film (6:4) was further tested under a series of static strains. Figure 3b shows that the water permeability slightly increased from 1.6 ± 0.18 to 2.9 ± 0.1 g $m^{-2}day^{-1}$ as the strain increased from 0 to 50%. This could be attributed to the small thickness reduction. Nevertheless, the generally low H_2O adsorption and diffusion ensured the very low water permeability compared to other materials.

The unique combination of high flexibility and low water permeability brought a substantial advantage for the PIB blend films to be used as a stretchable packaging material for flexible NGs. To demonstrate this advantage, a scatter plot was constructed to compare the modulus and water permeability of our PIB blend film to other state-of-the-art commercial or literature-reported packaging materials (Figure 3c).[29–34] It can be clearly seen that the PIB blend film from this work resides uniquely at the lower left corner. Ecoflex, a commercial elastomer with a similar modulus, had substantially higher water permeability. Typical water-insulating packaging materials, such as PHB, PP, and LDPE, had similar levels of water permeability, but their moduli are all in the GPa range, ~3 to 5 orders of magnitude higher than our PIB blends. This comparison demonstrated that only our PIB blends can satisfy both high water resistance and tissuelike mechanical property requirements simultaneously for the development of implantable NGs. As the PIB blends were designed to act as a flexible packaging material for implantable medical devices, the biocompatibility of the PIB blend films (6:4) was also evaluated. First, the biocompatibility of the PIB blend was studied by incubating and comparing mouse aortic smooth muscle (MOVAS) cells with and without (control) PIB blend films. Immunofluorescence staining images showed that the cells incubated with PIB had typical elongated morphology together with appropriate distributions and densities, exhibiting no difference compared to the cells in the control group (Figure 3d). The CellTiter-Glo (CTG) assay was further performed to quantitatively

evaluate the survival of MOVAS in contact with the material. As shown in Figure 3e, the cell viability on PIB blend films (92.3%) did not exhibit a significant difference compared to the control group (100%). These results confirmed the nontoxicity of the PIB blend film, indicating its ideal role as biocompatible packaging material.

To demonstrate the unique advantage of the PIB blend packaging material, a simple sliding-mode TENG was fabricated and packaged by PIB blend films. As schematically shown in Figure 4a, the sliding-mode TENG had the following two parts: a central mobile layer made from the Cu film and top/bottom stationary layers composed of a PTFE film covered by a Cu electrode. The entire TENG was completely packaged by a 300 μm PIB blend film with each side kept at ~3 mm from the TENG device. The PIB blend film was tightly attached to the Cu electrode surface and the front portion of the central mobile layer surface by hot pressing. Two centimeters between the fixing areas on the Cu electrode and the mobile layer was left unattached, forming a stretchable cavity allowing free lateral movement of the central mobile layer. The packaged TENG was operated by pulling the central mobile layer back and forth, and the output voltage was measured from Cu electrodes (the working mechanism of this sliding-mode TENG is shown in Figure S7). To compare the performance of PIB blends, the same TENGs with the same voltage output were packaged by another three common packaging elastomers, i.e., Ecoflex, PDMS, and polyethylene (PE). All of the package layers had the same size and thickness.

All of the TENGs were first tested under the same pulling force of ~0.49 N (setup details are given in Figure S8). The asymmetric voltage peaks from TENGs were induced by the different movement speeds of forward pulling and backward retracting of the TENG devices during the tests. Due to the different elastic moduli of the packaging materials, the same pulling force induced different levels of displacement (strain) at the stretchable cavity, where the PIB blend-packaged TENG demonstrated the highest strain of 45%. Accordingly, it also generated the highest voltage output with a peak-to-peak value (V_{pp}) of ~2.2 V (Figure 4b). Ecoflex, with a slightly higher modulus, exhibited a close strain of 40% and a slightly lower V_{pp} of ~1.6 V. The strain and V_{pp} drastically dropped to 5.5% and ~0.8 V, respectively for the PDMS-packaged TENG as its modulus was 16 times higher than that of the PIB blend film. The much more rigid PE (1.5 GPa) package yielded negligibly low strain and voltage outputs. This comparison clearly revealed the significance of a low elastic modulus for the packaging material for the operation of flexible implantable NGs, as the available driving force from body tissue movements is rather limited. Considering the practical application conditions of implantable NGs, the long-term protection of the PIB blend was evaluated under continuous dynamic deformation. Figure 4c shows the recorded voltage output profiles of the PIB blend-packaged TENG over 15 days. The device was repeatedly stretched to a 30% strain and released at 1 Hz in deionized water. The day 0 signal was voltage outputs measured before soaking in water. It can be clearly seen that the device was able to retain its original output for 2 weeks, demonstrating an excellent water barrier property and electric resistance of PIB blends. The output dropped to zero on day 15. It was because of the wearing out of the contacting point with the anchoring base that was needed for the in-water straining test (Figure S9). A much longer protection period can be expected in practical applications when no ridge anchoring points are involved. As Ecoflex offers the same level of flexibility as PIB blends, a comparison was conducted

on Ecoflex-packaged TENGs under the same testing conditions. As shown in Figure 4d, the voltage output dropped drastically after immersing in water for just 2 days and the device completely failed on day 3. The time-dependent V_{pp} values of both PIB blend and Ecoflex-packaged TENGs are plotted in Figure 4e. It clearly revealed that the PIB blend films were able to offer substantially longer and stable protection than Ecoflex under a dynamic straining action in an aqueous environment.

CONCLUSIONS

In summary, this work presents a PIB blend-based packaging material that simultaneously offers a tissue-like elastic modulus and an excellent dynamic water resistivity. Young's modulus of PIB blends was reduced from pristine H-PIB (M_n = 600 000, ~400 kPa) by mixing with L-PIB (M_n = 920) and reached an optimal value of ~62 kPa at a L- to H-PIB weight ratio of 6:4. The PIB blends film also exhibited an excellent water barrier property. The water permeability was found as low as 1.6 ± 0.18 g m^{-2} day^{-1} for the PIB blend film at 6:4, more than two orders of magnitude lower than those of other common packaging elastomers, such as Ecoflex and PDMS. In addition, the water permeability only slightly increased to 2.9 ± 0.1 g $m^{-2}day^{-1}$ when the film was under a high strain of 50%. Other typical packaging materials with similar levels of water permeability, such as PHB, LDPE, all have 3–5 orders of magnitude higher moduli in the GPa range. The unique combination of excellent flexibility and extremely low water permeability was attributed to the nonpolar C chain and the small and dense pendant methyl groups that offer low H_2O adsorption and diffusion while retaining good chain mobility. This property allowed the PIB blend film to be used as a packaging material for flexible IMDs. To demonstrate this capability, sliding-mode TENGs were packaged by the PIB blend film and operated in water. PIB-packaged TENG demonstrated a stable in-water electrical output work over a 14-day testing period, substantially outperforming the Ecoflex-packaged TENG that only lasted for 2 days. While the technology readiness level is still very early, this work suggests a practical solution for packaging flexible IMDs, such as implantable NGs that need to operate in a physiological environment and are subject to constant straining actions.

EXPERIMENTAL SECTION

Preparation of PIB Blend Films.

High-molecular-weight PIB (H-PIB, M_n:600 000) and low-molecular-weight PIB (L-PIB, M_n:920) were supplied by Sigma. PIB blend films with different weight ratios of 2:8, 3:7, 4:6, 5:5, 6:4, and 7:3 (L-PIB:H-PIB) were prepared by solution blending in hexane and stirred for 4 h to obtain a homogeneous mixture. The mixture was cast on a Petri dish surface to a defined thickness. The mixture films were dried in an atmosphere at room temperature until whole solvent was completely evaporated and transparent PIB blend films were achieved.

Fabrication of Sliding-Mode TENGs with Package.

The PTFE film and Cu film was used as the triboelectric layers to fabricate a sliding-mode TENG. PET (0.7 × 3.5 cm^2, 300 μm thickness, CS Hyde Company) was used as the

substrate, and Cu tape (100 μm) was attached to both sides of the PET film to act as the mobile layer. A thin PTFE film (2.5 × 1 cm^2, 50 μm, CS Hyde Company) with an attached Cu electrode was used as the static part. The sliding-mode TENG was assembled by attaching two PTFE/Cu films along the edges with the PTFE surface facing each other. The Cu/PET/Cu mobile layer was inserted in between the two PTFE/Cu films.

The PIB blend film with a weight ratio of 6:4 was used to package the sliding-mode TENGs. A thin film of Ecoflex (Reynolds Advanced Materials, Inc., 30–40 μm in thickness) was also coated outside of PIB. The total package film has a thickness of 300 μm. The edge was sealed by hot compression at a temperature of 140 °C. For comparison, the same TENGs were also packaged by 300 μm Ecoflex. The Ecoflex film was made by spin-coating a solution consisting of parts A and B (1:1 by weight) at a speed of 500 rpm for 30 s. As a result, the Ecoflex film with a thickness of ~300 μm was achieved. The film was wrapped around the TENG, and uncured Ecoflex solution was applied to the joint edge for adhesion. The edges of the PIB and Ecoflex films were sealed together by hot compression at a temperature of 90 °C, leaving the middle part unattached. The TENG device in the middle pushes up the PIB film, naturally forming a cavity that allows the slide layer to move freely.

Mechanical Property Measurement.

The static tensile properties, dynamic modulus, and temperature sweep measurements were performed by an RSA III dynamic mechanical analyzer using a rectangular geometry. All of the films for mechanical property testing were made in a rectangular shape with a size of 30 × 7 mm^2 and a thickness of 300 μm. The static tensile properties were characterized at room temperature at a strain rate of 50 mm min^{-1}. The stress–strain curves were measured using a transient force gap method. Three tests were conducted for each film, and the error bars represent ± standard deviation (n = 3). The dynamic moduli were measured at the frequency of 1 Hz at room temperature within a strain range from 1 to 10%. Two tests were conducted for each film. For temperature sweep measurement, the films were fixed on a tension clamp and strained to 0.1% at a frequency of 1 Hz, where the temperature was swept from −90 to 0 °C at a heating rate of 2.5 °C min^{-1}.

Fourier Transform Infrared (FTIR) Spectrometry.

The FTIR spectra of the pristine H-PIB film and PIB (6:4) blend film were measured by a Nicolet iS50R FTIR spectrophotometer.

Water Contact Angle Measurement.

The contact angles of water droplets on the material surfaces were measured using a contact angle system at room temperature. Deionized water droplets (5 μL) were applied to the film surface by the automatic dispenser of the contact angle system. The contact angles were determined from the side-view images of dispensed water droplets.

Water Transmission Rate.

The gravimetric method was used to determine the water transmission rates of all of the films at room temperature. The setup of this measurement is shown in Figure S5. The film samples were placed over the mouth of vials prefilled with anhydrous copper sulfate. The

film edges were sealed by a paraffin film to the mouth of vials and further tightened by a hollow lid. All of the vials have a diameter of 1 cm. After applying the film, the vial was placed in a beaker filled with DI water for three weeks. The vial was then removed from water, and its weight increment was measured immediately. The water transmission rate was calculated using the following equation: WTR = $\Delta m/A/t$, where Δm is the weight increment of the vial (g), A is the exposed film surface area (m^2), and t is the total time being immersed in water (day). Three tests were conducted for each type of film. The mean value was reported, and the error bars represented ±standard deviation ($n = 3$).

Output Performance Measurement of Packaged TENGs.

The output performance of packaged TENGs was measured under the same pulling force. TENGs with the same voltage output were packaged by the PIB blend film, Ecoflex, PDMS, and PE, respectively. All of the package films had the same size and thickness. The experimental setup is shown in Figure S8. To achieve the same pulling force, a 50 g weight was affixed at the front tip of the central mobile layer by a thread. The nonmobile part of the device was attached to a fixed stand, and the weight was placed on the edge of the stand. During the test, the weight was released to create a free-fall motion. Through the same falling distance until the string was pulled straight, the same amount of pulling force can be expected on the mobile layer of TENG. Based on their different stretchabilities, the packaging materials were stretched to different lengths. Correspondingly, the mobile layer moved different distances, generating different amounts of electrical outputs. The voltage outputs of the four packaged devices were measured by a multimeter (DMM 6500, Keithley, internal resistance 10 MΩ). The strain of the packaging material was determined by $(L - L_0)/L_0 \times 100$, where L_0 and L are the lengths before and after the packaging material was stretched, respectively. The force of the falling weight was given by the mass of the weight via $F = mg$, where g is the acceleration due to gravity.

Dynamic Waterproof Performance Evaluation.

The dynamic waterproof performance of the PIB blend films as a packaging material was characterized by measuring the time-dependent outputs of packaged TENGs in water. The output voltage was measured by a multimeter (DMM 6500, Keithley, internal resistance 10 MΩ) from the TENG when it was strained in water. The static parts of TENG were fixed on a stationary stage located at the bottom of a container filled with water. The mobile layer was attached to a moveable stage, which was connected to a computer-controlled linear motor. The entire TENG was completely immersed in water. During the measurement, the mobile layer was pulled back and forth periodically for 1 cm at a frequency of 1 Hz. The TENG operation was kept on for 5 h each day, and the voltage output was recorded at the end of the operation. The TENG was immersed in water all of the time even when it was not in operation.

Cell Morphology Examination.

UV-sterilized samples of the PIB blend were placed on the inside of the walls of a chambered cell culture slide (Falcon 354108). No material was added to the control wells. There were four wells in each group. In total, 2.5×10^4 MOVAS cells were seeded into each well containing 500 μL of cell culture medium. After 48 h, the cytoskeleton and

nucleus of the cells were stained with Alexa Fluor 555 Phalloidin (Thermo Fisher Scientific, A34055) and DAPI, respectively. The staining protocol includes the following procedures: first, the cell culture medium was discarded and cells were washed two times with PBS. They were later fixed with 4% paraformaldehyde for 15 min and rinsed three times with PBS. The cell samples were then permeabilized with 0.1% Triton X-100 for 15 min at room temperature and rinsed three times with PBS. The samples were incubated for 30 min at room temperature with 200 μL well^{-1} of Alexa Fluor 555 Phalloidin working solution and then washed three times with PBS. Finally, a fluorescent mounting medium with DAPI (GBI Labs, E19-100) was added and incubated for 5 min at room temperature before applying a coverslip. After staining, the cells were imaged using a Nikon A1RS high-definition (HD) confocal microscope.

Biocompatibility Evaluation.

MOVAS cells were purchased from American Type Culture Collection (ATCC, CRL-2797) and grown as recommended in modified DMEM containing 4.5 g L^{-1} D-glucose (Thermo Scientific, 11965118) supplemented with 10% fetal bovine serum (FBS), 100 U mL^{-1} penicillin, and 100 U mL^{-1} streptomycin. The cell biocompatibility of the PIB blend was assessed with a CellTiter-Glo assay (Promega, G9242) as described.[35] UV-sterilized samples of the PIB blend were placed on the inside of the walls of a 96-well plate with a black wall and clear bottom (Corning 3603). No material was added to the control wells. There were three wells in each group. In total, 5×10^3 cells were seeded into each well containing 200 μL of cell culture medium. After incubation for 48 h at 37 °C and 5% CO_2, the cell culture medium was aspirated and 100 μL of PBS and 100 μL of CellTiter-Glo solution were added to each well followed by incubation at room temperature for 30 min. Luminescence was recorded on a FlexStation 3 microplate reader (Molecular Devices) at an integration time of 0.5 s well^{-1}. The relative cell viability was expressed as (luminescence of sample wells-blank) (luminescence of control wells-blank) × 100%, where blank is the luminescence of the wells without cells (PBS and CellTiter-Glo solution only).

Supplementary Material

Refer to Web version on PubMed Central for supplementary material.

ACKNOWLEDGMENTS

This work was supported by the National Institutes of Health under Award Number R01HL157077. The content is solely the responsibility of the authors and does not necessarily represent the official views of the National Institutes of Health. Y.S. acknowledges support from the China Scholarship Council, China (CSC, File No. 201906240140)

REFERENCES

(1). Cobelli N; Scharf B; Crisi GM; Hardin J; Santambrogio L Mediators of the Inflammatory Response to Joint Replacement Devices. Nat. Rev. Rheumatol. 2011, 7, 600–608. [PubMed: 21894210]

(2). Yu X; Wang H; Ning X; Sun R; Albadawi H; Salomao M; Silva AC; Yu Y; Tian L; Koh A; Lee CM; Chempakasseril A; Tian P; Pharr M; Yuan J; Huang Y; Oklu R; Rogers JA Needle-Shaped Ultrathin Piezoelectric Microsystem for Guided Tissue Targeting via Mechanical Sensing. Nat. Biomed. Eng. 2018, 2, 165–172. [PubMed: 31015715]

(3). Long Y; Wei H; Li J; Yao G; Yu B; Ni D; Gibson AL; Lan X; Jiang Y; Cai W; Wang X Effective Wound Healing Enabled by Discrete Alternative Electric Fields from Wearable Nanogenerators. ACS Nano 2018, 12, 12533–12540. [PubMed: 30488695]

(4). Yang F; Li J; Long Y; Zhang Z; Wang L; Sui J; Dong Y; Wang Y; Taylor R; Ni D; Cai W; Wang P; Hacker T; Wang X Wafer-Scale Heterostructured Piezoelectric Bio-Organic Thin Films. Science 2021, 373, 337–342. [PubMed: 34437153]

(5). Nichols SP; Koh A; Storm WL; Shin JH; Schoenfisch MH Biocompatible Materials for Continuous Glucose Monitoring Devices. Chem. Rev. 2013, 113, 2528–2549. [PubMed: 23387395]

(6). Burri H; Senouf D Remote Monitoring and Follow-up of Pacemakers and Implantable Cardioverter Defibrillators. Europace 2009, 11, 701–709. [PubMed: 19470595]

(7). Keppeler D; Schwaerzle M; Harczos T; Jablonski L; Dieter A; Wolf B; Ayub S; Vogl C; Wrobel C; Hoch G; Abdellatif A; Jeschke M; Rankovic V; Paul O; Ruther P; Moser T Multichannel Optogenetic Stimulation of the Auditory Pathway Using Microfabricated LED Cochlear Implants in Rodents. Sci. Transl. Med. 2020, 12, No. eabb8086. [PubMed: 32718992]

(8). Pons-Faudoa FP; Ballerini A; Sakamoto J; Grattoni A Advanced Implantable Drug Delivery Technologies: Transforming the Clinical Landscape of Therapeutics for Chronic Diseases. Biomed. Microdevices. 2019, 21, No. 47. [PubMed: 31104136]

(9). Wang C; Liu Y; Qu X; Shi B; Zheng Q; Lin X; Chao S; Wang C; Zhou J; Sun Y; Mao G; Li Z Ultra-Stretchable and Fast Self-Healing Ionic Hydrogel in Cryogenic Environments for Artificial Nerve Fiber. Adv. Mater. 2022, No. 2105416.

(10). Wang C; Qu X; Zheng Q; Liu Y; Tan P; Shi B; Ouyang H; Chao S; Zou Y; Zhao C; Liu Z; Li Y; Li Z Stretchable, Self-Healing, and Skin-Mounted Active Sensor for Multipoint Muscle Function Assessment. ACS Nano 2021, 15, 10130–10140. [PubMed: 34086454]

(11). Chen K; Ren J; Chen C; Xu W; Zhang S Safety and Effectiveness Evaluation of Flexible Electronic Materials for Next Generation Wearable and Implantable Medical Devices. Nano Today 2020, 35, No. 100939.

(12). Byun J; Lee Y; Yoon J; Lee B; Oh E; Chung S; Lee T; Cho K-J; Kim J; Hong Y Electronic Skins for Soft, Compact, Reversible Assembly of Wirelessly Activated Fully Soft Robots. Sci. Rob. 2018, 3, No. eaas9020.

(13). Liu Z; Ma Y; Ouyang H; Shi B; Li N; Jiang D; Xie F; Qu D; Zou Y; Huang Y; Li H; Zhao C; Tan P; Yu M; Fan Y; Zhang H; Wang ZL; Li Z Transcatheter Self-Powered Ultrasensitive Endocardial Pressure Sensor. Adv. Funct. Mater. 2019, 29, No. 1807560.

(14). Yao G; Kang L; Li J; Long Y; Wei H; Ferreira CA; Jeffery JJ; Lin Y; Cai W; Wang X Effective Weight Control via an Implanted Self-Powered Vagus Nerve Stimulation Device. Nat. Commun. 2018, 9, No. 5349. [PubMed: 30559435]

(15). Zhao C; Feng H; Zhang L; Li Z; Zou Y; Tan P; Ouyang H; Jiang D; Yu M; Wang C; Li H; Xu L; Wei W; Li Z Highly Efficient in Vivo Cancer Therapy by an Implantable Magnet Triboelectric Nanogenerator. Adv. Funct. Mater. 2019, 29, No. 1808640.

(16). Zheng Q; Jin Y; Liu Z; Ouyang H; Li H; Shi B; Jiang W; Zhang H; Li Z; Wang ZL Robust Multilayered Encapsulation for High-Performance Triboelectric Nanogenerator in Harsh Environment. ACS Appl. Mater. Interfaces. 2016, 8, 26697–26703. [PubMed: 27696802]

(17). Li J; Kang L; Long Y; Wei H; Yu Y; Wang Y; Ferreira CA; Yao G; Zhang Z; Carlos C; German L; Lan X; Cai W; Wang X Implanted Battery-Free Direct-Current Micro-Power Supply from in Vivo Breath Energy Harvesting. ACS Appl. Mater. Interfaces. 2018, 10, 42030–42038. [PubMed: 30444344]

(18). Zheng Q; Zhang H; Shi B; Xue X; Liu Z; Jin Y; Ma Y; Zou Y; Wang X; An Z; Tang W; Zhang W; Yang F; Liu Y; Lang X; Xu Z; Li Z; Wang ZL In Vivo Self-Powered Wireless Cardiac Monitoring via Implantable Triboelectric Nanogenerator. ACS Nano 2016, 10, 6510–6518. [PubMed: 27253430]

(19). Li J; Kang L; Yu Y; Long Y; Jeffery JJ; Cai W; Wang X Study of Long-Term Biocompatibility and Bio-Safety of Implantable Nanogenerators. Nano Energy 2018, 51, 728–735. [PubMed: 30221128]

(20). Puskas JE; Chen Y Biomedical Application of Commercial Polymers and Novel Polyisobutylene-based Thermoplastic Elastomers for Soft Tissue Replacement. Biomacromolecules 2004, 5, 1141–1154. [PubMed: 15244424]

(21). George SC; Thomas S Transport Phenomena Through Polymeric Systems. Prog. Polym. Sci. 2001, 26, 985–1017.

(22). Vohra A; Filiatrault HL; Amyotte SD; Carmichael RS; Suhan ND; Siegers C; Ferrari L; Davidson GJE; Carmichael TB Reinventing Butyl Rubber for Stretchable Electronics. Adv. Funct. Mater. 2016, 26, 5222–5229.

(23). Tenn N; Follain N; Fatyeyeva K; Poncin-Epaillard F; Labrugère C; Marais S Impact of Hydrophobic Plasma Treatments on the Barrier Properties of Poly(lactic acid) Films. RSC Adv. 2014, 4, 5626–5637.

(24). Chen J; Peng Q; Thundat T; Zeng H Stretchable, Injectable, and Self-Healing Conductive Hydrogel Enabled by Multiple Hydrogen Bonding toward Wearable Electronics. Chem. Mater. 2019, 31, 4553–4563.

(25). Wu J; Huang G; Wang X; He X; Xu B Changes in the Viscoelastic Mechanisms of Polyisobutylene by Plasticization. Macromolecules 2012, 45, 8051–8057.

(26). Xia L; Li C; Zhang X; Wang J; Wu H; Guo S Effect of Chain Length of Polyisobutylene Oligomers on the Molecular Motion Modes of Butyl Rubber: Damping Property. Polymer 2018, 141, 70–78.

(27). Marcano A; Fatyeyeva K; Koun M; Dubuis P; Grimme M; Marais S Recent Developments in the Field of Barrier and Permeability Properties of Segmented Polyurethane Elastomers. Rev. Chem. Eng. 2019, 35, 445–474.

(28). Boyd RH; Pant PK Molecular Packing and Diffusion in Polyisobutylene. Macromolecules 1991, 24, 6325–6331.

(29). Chaos A; Sangroniz A; Gonzalez A; Iriarte M; Sarasua J-R; del Río J; Etxeberria A Tributyl Citrate as an Effective Plasticizer for Biodegradable Polymers: Effect of Plasticizer on Free Volume and Transport and Mechanical Properties. Polym. Int. 2019, 68, 125–133.

(30). Sangroniz L; Ruiz JL; Sangroniz A; Fernández M; Etxeberria A; Müller, A. J.; Santamaria, A. Polyethylene Terephthalate/Low Density Polyethylene/Titanium Dioxide Blend Nanocomposites: Morphology, Crystallinity, Rheology, and Transport Properties. J. Appl. Polym. Sci. 2019, 136, No. 46986.

(31). Selbmann F; Baum M; Wiemer M; Gessner T In Depositionof Parylene C and Characterization of its Hermeticity for the Encapsulation of MEMS and Medical Devices, 2016 IEEE 11th Annual International Conference on Nano/Micro Engineered and Molecular Systems (NEMS), IEEE, 2016; pp 427–432.

(32). Huang W; Zeng S; Liu J; Sun L Bi-axially Oriented Polystyrene/Montmorillonite Nanocomposite Films. RSC Adv. 2015, 5, 58191–58198.

(33). Thanakkasaranee S; Kim D; Seo J Preparation and Characterization of Polypropylene/Sodium Propionate (PP/SP) Composite Films for Bread Packaging Application. Packag. Technol. Sci. 2018, 31, 221–231.

(34). Monprasit P; Ritvirulh C; Sooknoi T; Rukchonlatee S; Fuongfuchat A; Sirikittikul D Selective Ethylene-Permeable Zeolite Composite Double-Layered Film for Novel Modified Atmosphere Packaging. Polym. Eng. Sci. 2011, 51, 1264–1272.

(35). Zhou T; Wang W; Phan N; Ren J; Yang H; Feldman CC; Feltenberger JB; Ye Z; Wildman SA; Tang W; Liu B Identification of a Novel Class of RIP1/RIP3 Dual Inhibitors that Impede Cell Death and Inflammation in Mouse Abdominal Aortic Aneurysm Models. Cell Death Dis. 2019, 10, No. 226. [PubMed: 30842407]

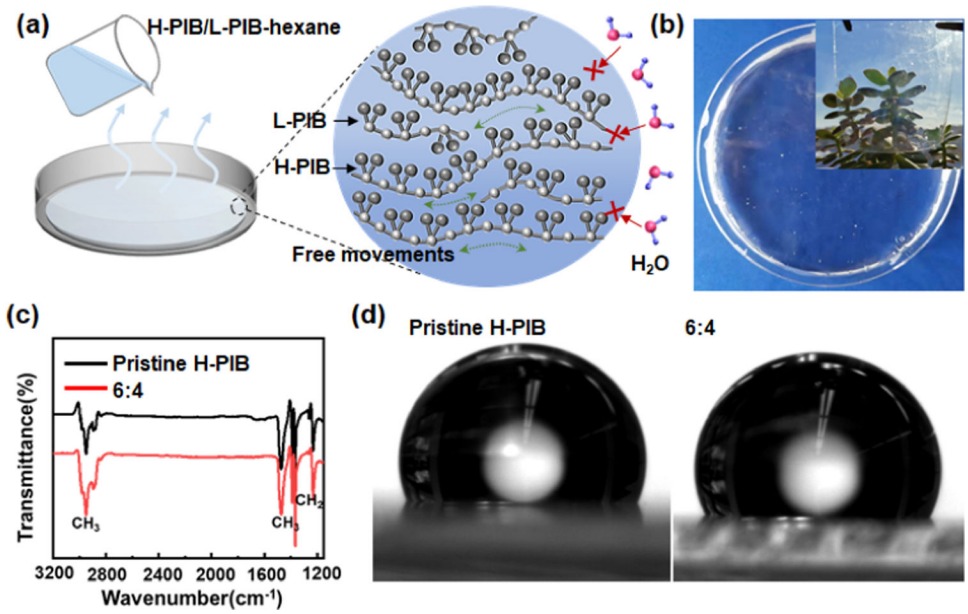

Figure 1.

PIB blend film design and basic properties. (a) Schematic processing of the PIB blend film. The inset shows the mixing interaction of L-PIB and H-PIB. (b) Digital photo of an as-prepared PIB blend film with high transparency. (c) FTIR spectra of pristine H-PIB and PIB blend (6:4) films showing identical characteristic absorption peaks. (d) Comparison of water contact angles of pristine H-PIB (right) and PIB blend (6:4) films (left) showing a negligible change in the material hydrophobicity.

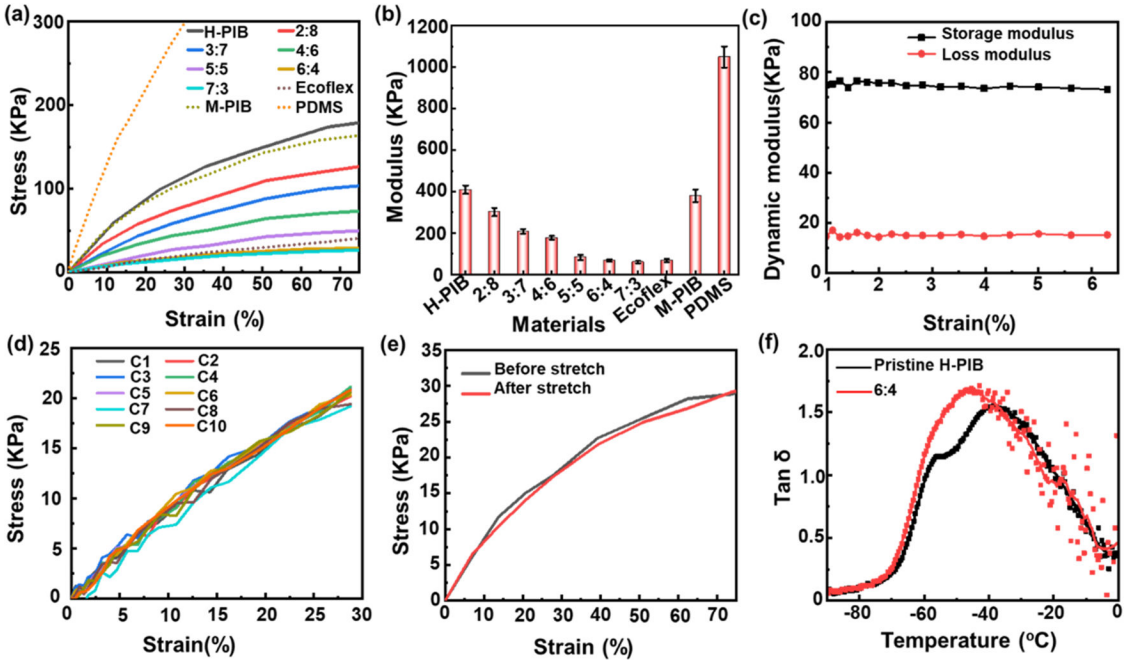

Figure 2.

Mechanical properties of PIB blend films. (a) Tensile strain–stress curves and (b) corresponding elastic modulus (determined at <30% strain) of PIB blends with different mixing ratios and other benchmark samples including Ecoflex, PDMS, and M-PIB (M_n = 200 000); (c) dynamic mechanical properties; (d) tensile stress–strain curves in ten cycles at 30% strain during loading–unloading cycles of the PIB blend film (6:4); (e) tensile strain–stress curves before and after stretching in water for 18 000 times; and (f) tan δ spectra of PIB blend films.

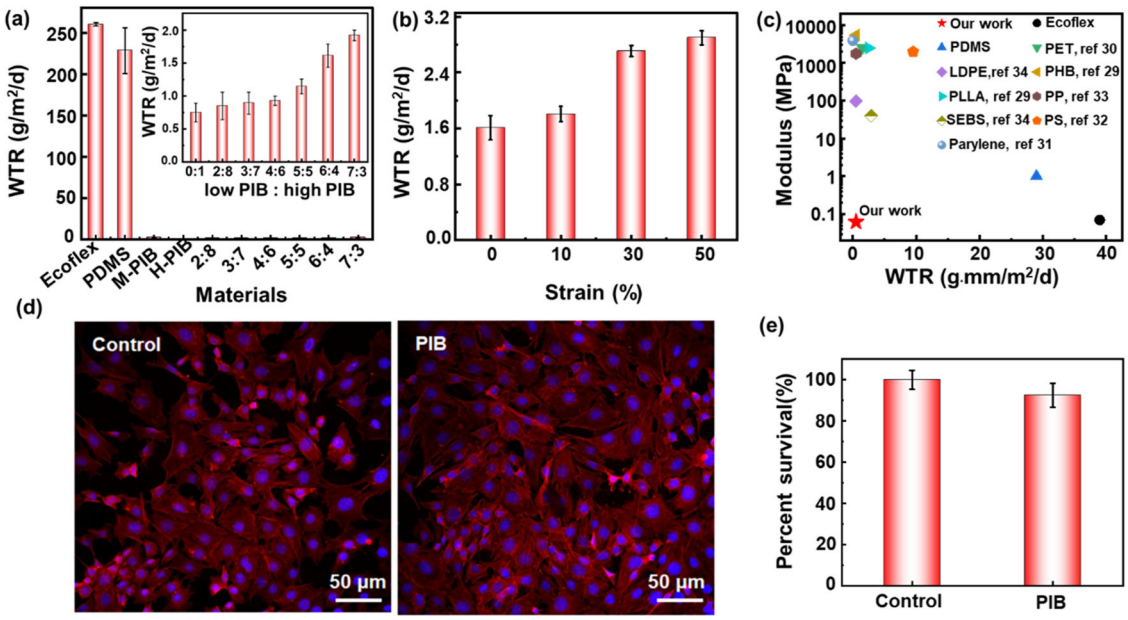

Figure 3.

Water permeability characterization and comparison. (a) Water permeability measured at 0% strain from PIB blend films with different ratios in comparison to other commercial packaging elastomers; the inset is an enlarged scale from (a) to show the water permeability of all PIB blend films. (b) Water permeability of the PIB blend film (6:4) measured at different strains. (c) Comparison of modulus and water permeability of the PIB blend film with those of commonly used packaging materials. (d) Fluorescence microscopy image of MOVAS cells stained by Alexa Fluor 555 Phalloidin and DAPI. (e) Viability of cells after 48 h exposure to PIB blend film extraction media.

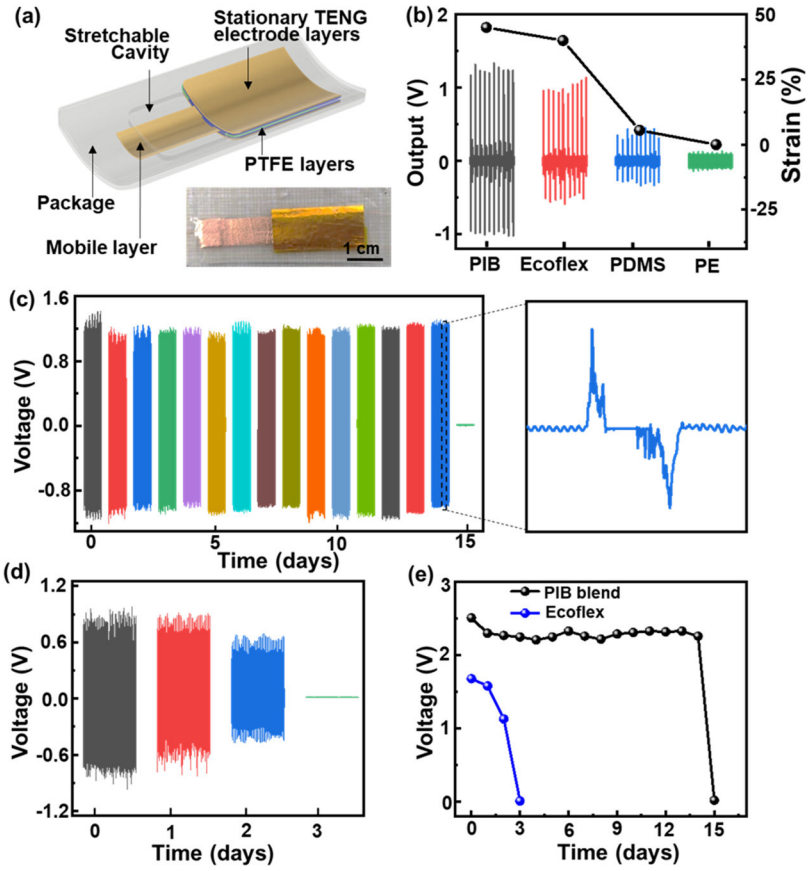

Figure 4.

Performance of PIB blend-packaged TENG. (a) Schematic structure of a simple sliding-mode TENG packaged by PIB blend films; the inset is the digital photo of a packaged TENG. (b) Voltage output of the same type of TENG packaged by four different elastomers when subjected to the same amount of tensile strain. (c, d) Long-term in-water voltage output of TENG packaged by the PIB blend (c) and Ecoflex (d). The insert of (c) is an enlarged voltage output profile within one stretching cycle. (e) Comparison of time-dependent peak-to-peak voltage output of TENG packaged by the PIB blend and Ecoflex.